

New insights into the source of gold in the Youjiang basin, SW China

Jun Chen^{1,6}, Li-Juan Du¹, Rui-Dong Yang¹, Mei-Fu Zhou^{2,3}, Chun-Kit Lai^{4,5}, and Zhi-Long Huang^{2,†}

¹College of Resources and Environmental Engineering, Guizhou University, Guiyang 550025, P.R. China

²State Key Laboratory of Ore Deposit Geochemistry, Institute of Geochemistry, Chinese Academy of Sciences, Guiyang 550002, P.R. China

³Department of Earth Sciences, The University of Hong Kong, Hong Kong, China

⁴Faculty of Science, Universiti Brunei Darussalam, Gadong, Brunei

⁵Fortescue Metals Group Ltd., East Perth WA 6004, Australia

⁶Key Laboratory of Karst Georesources and Environment, Ministry of Education, Guizhou University, Guiyang 550025, China

ABSTRACT

Mantle plume rich in gold is considered to be important for the formation of giant epigenetic gold deposits. The Youjiang basin, SW China, is the world's second largest Carlin-type gold province, but the ultimate source of its gold remains enigmatic. In this study, we report that the Middle–Late Permian basaltic rocks in the basin are rich in native gold grains. These gold grains are scattered in the interstices of pyrite and marcasite and in the amorphous silica cavities. Mineralogy and S–Pb isotope geochemistry of the auriferous sulfides suggest that the gold was largely derived from the gold-rich Late Permian (ca. 260 Ma) Emeishan plume and was released to a near-surface volcanogenic massive sulfide (VMS) metallogenic system, where it accumulated. The native gold grains from the basalts may have been inherited by the younger (ca. 140 Ma) Carlin-type ores in the Youjiang basin, which are indicative of gold pre-enrichment in the basin. Our study highlights that golden plume upwelling could carry abundant gold into the upper crust, even into shallow-level metallogenic systems, and thus provides an alternative view on the source of gold in the Youjiang basin.

INTRODUCTION

Carlin-type gold deposits represent a major gold resource of the world and are mainly distributed in Nevada, USA, (Cline et al., 2005) and SW China (Su et al., 2018), notably in the Youjiang basin, which has >800 metric tonnes (mt) of Au resource (Wang and Groves, 2018). However, the ultimate source of gold has been

debated for many decades. Although stable isotopes (C–H–O–S) can be used to determine the ore–fluid origin (Su et al., 2018; Zhuo et al., 2019; Li et al., 2020), the origin of gold is difficult to determine. The gold source of the Youjiang basin has been interpreted as sedimentary (Yan et al., 2018), metamorphic (Su et al., 2009, 2012; Li et al., 2020), and/or magmatic (Xie et al., 2018).

High gold contents of source rocks can be a key factor in world-class gold ore formation (Bierlein and Pisarevsky, 2008; Pitcairn, 2011; Webber et al., 2013). Mantle plumes that originated from the lower mantle or core–mantle boundary may carry siderophile elements into the upper mantle and the crust (Keays and Scott, 1976; Brandon and Walker, 2005; Bierlein and Pisarevsky, 2008; Tassara et al., 2017). Consequently, golden plumes (gold-rich mantle, as defined by Webber et al., 2013) may promote gold mineralization (Tassara et al., 2017). In some cases, gold is transported as a distinct metal phase in mantle-derived magmas in large igneous provinces or mantle hotspots, such as the Emeishan picritic basalts (ca. 260 Ma; Zhang et al., 2006a) and Hawaiian lavas (Sisson, 2003). The Youjiang basin in the Emeishan large igneous province outer zone (Fig. 1A) is the host of many Carlin-type Au deposits. Gold deposits in this basin are mostly hosted in Middle–Upper Permian carbonaceous rocks (Su et al., 2018) and Emeishan volcanic rocks (Fig. 1B; Chen et al., 2018; Hu et al., 2018; Zhu et al., 2020; Li et al., 2021). Although a few studies proposed an ambiguous link between the Emeishan large igneous province and the Carlin-type Au mineralization (Zhu et al., 2020), this hypothesis has not received strong support due to inadequate data, particularly for evidence of golden plume involvement in the basin.


In this study, we report on native gold grains from the unaltered Middle–Upper Permian submarine basaltic rocks in the Youjiang basin. This

finding supports the transport of gold to the shallow crustal volcanogenic massive sulfide (VMS) mineralization system by mantle plume-derived mafic magmas. We discuss the genetic link between the Emeishan plume and gold mineralization in the basin and support the view on gold pre-enrichment for the later Carlin-style gold mineralization.

GEOLOGICAL BACKGROUND

Emeishan Large Igneous Province and Ore Deposits

The Emeishan large igneous province covers an area of over ~500,000 km² (Xu et al., 2004) and contains voluminous pillow basalts and mafic hyaloclastite (tuff) deposits in the early eruptive stages, and in the late eruptive phases it contains subsequent terrestrial flood basalts (Jerram et al., 2016; Zhu et al., 2018, 2021), picrites, mafic-ultramafic intrusions, and felsic rocks (trachyte and rhyolite) (Ali et al., 2005; Yao et al., 2019; Yan et al., 2020). The thickness of the volcanic piles ranges from several meters (Emeishan large igneous province outer zone; Fig. 1A) to over 5 km (Emeishan large igneous province inner zone; Zhu et al., 2018). Based on high-precision secondary ion mass spectrometry (SIMS) and chemical abrasion–thermal ionization mass spectrometry (CA–TIMS) zircon U–Pb dating, the main phase of the Emeishan flood basalt eruption occurred at ca. 260–259 Ma (Zhu et al., 2021). The Emeishan mantle plume may have contributed the heat and metals to form various basalt-hosted Cu (Mao et al., 2003), magmatic Fe–Ti–V oxide (e.g., Taihe, Baima, and Hongge deposits; Tao et al., 2007; Zhang et al., 2009; Hou et al., 2011), and magmatic Cu–Ni(–PEG) sulfide (Song et al., 2003) deposits in the region. Meanwhile, native gold blebs in fresh olivine phenocrysts from picritic lavas were reported at Lijiang in the Emeishan

Jun Chen  <https://orcid.org/0000-0001-5944-8561>

[†]Corresponding author: huangzhielong@vip.gyig.ac.cn.

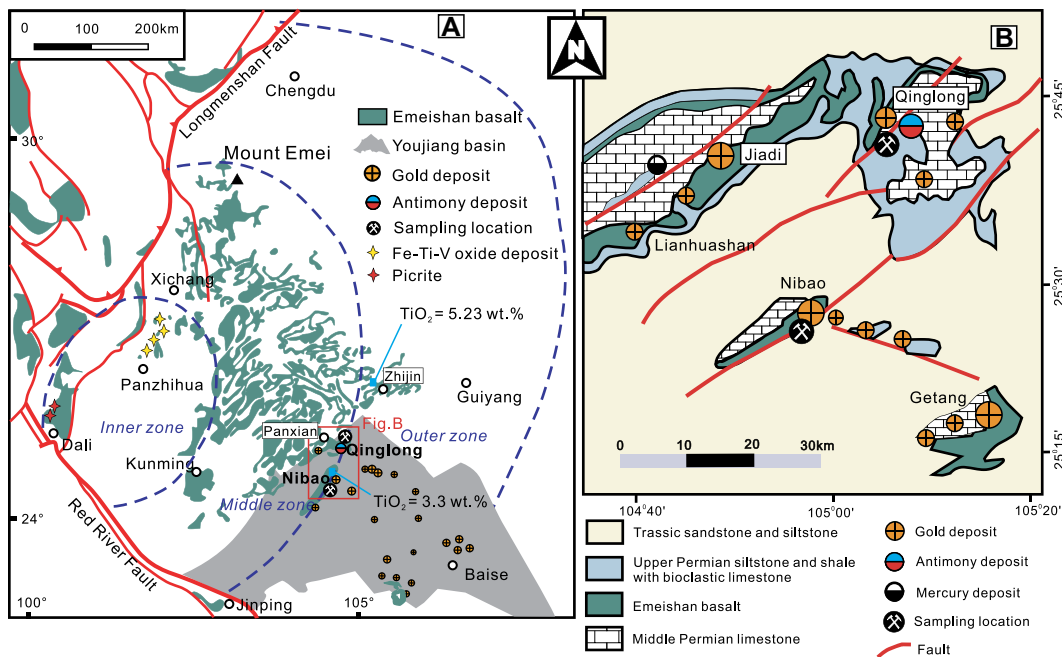


Figure 1. (A) Simplified geologic map of the Emeishan large igneous province (LIP) and Youjiang basin shows that the basin is located in the outer zone of the Emeishan LIP where distributions of Carlin-type Au deposits are present (modified after Shellnutt, 2014). The TiO_2 contents of basalt at Zhijin and Nibao are based on Zhu et al. (2020). (B) Emeishan basalt-hosted, Carlin-type Au deposits at Nibao, Lianhuashan, and Getang and Sb-Au deposit at Qinglong (modified after Chen et al., 2021).

large igneous province inner zone (Zhang et al., 2006a), which provides direct evidence for Au enrichment in the deep mantle.

In the Youjiang basin, gold mineralization has been defined by many authors as Carlin-type based on the host rocks, ore-forming temperature, ore-related alterations, and ore mineral assemblages (e.g., Hu et al., 2017; Xie et al., 2018; Wang and Groves, 2018). The Carlin-type Au deposits in the basin are characterized by anomalous enrichments in As, Sb, Hg, and Tl and occur in replacement-style orebodies in the Permian–Triassic platform-/basin-facies carbonate and clastic rocks (Hu et al., 2017). Magmatic sulfur for auriferous pyrites in these Carlin-type deposits was suggested by in situ sulfur isotope analysis (Xie et al., 2018). Age dating of the ore-related hydrothermal minerals (e.g., quartz, apatite, and rutile) has defined two gold mineralization episodes, i.e., ca. 200–230 Ma (Pi et al., 2017) and ca. 140 Ma (Chen et al., 2019), in the southern and northern margins of the Youjiang basin, respectively. Both are significantly younger than the ca. 260 Ma Emeishan large igneous province (Shellnutt et al., 2020, and references therein). Such lag time between the regional gold mineralization and the Emeishan large igneous province led many authors to suggest that they have no genetic link, although such a link is supported by melt thermodynamic modeling (that calculates the residual melt compositions of the plume-derived magmas; Zhu et al., 2020), which further implies that the juvenile lower crust beneath the Emeishan large igneous province was a potential Au reservoir.

Middle–Upper Permian Basaltic Rocks in the Youjiang Basin

In the Youjiang basin, Upper Devonian to Lower Cretaceous (ca. 142 Ma) carbonaceous sedimentary successions and basaltic rocks were deposited/emplaced in the basinal margin (Hu et al., 2017). Thick Emeishan flood basalt sequence is buried hundreds of meters beneath the basin and hosts several gold deposits, including the Nibao, Jiadi, Lianhuashan, Getang, and Qinglong deposits (Fig. 1B). Zhu et al. (2020) compiled the geochemical data from over 200 basaltic rock samples from the basin and showed that over 90% of the samples belong to the high-Ti series. A coeval sequence in the northern part of the basin comprises Mn-rich claystone, basalt, and chert, which were likely deposited in a submarine volcanic-geothermal setting during the early large igneous province volcanism (Zhong et al., 2014; Gao et al., 2018; Xu et al., 2021). Previous studies also indicate that the early pyroclastic eruption may have been submarine (e.g., Jerram et al., 2016; Zhu et al., 2021). Submarine mafic volcanoclastic rocks are interbedded with chert, which overlie the Middle Permian carbonate platform in the northern basinal margin (Yan et al., 2020). The basinal stratigraphic sequence indicates protracted extension and periodic volcanism, with the volcanism peaking in the Late Permian–Early Triassic. Similar volcanic rocks are widespread in the Youjiang basin and are dominated by tuff and claystone beds overlying the Middle–Permian Maokou Formation (Huang et al., 2016; Yan et al., 2020). Zircons from the claystone yielded a U–Pb age of ca. 262.5 Ma

(Yan et al., 2020), which predates the subaerial Emeishan large igneous province eruptive phase.

In the Youjiang basin, a few submarine basaltic volcanic centers were found in the Middle Permian carbonate platform, as indicated by volcanic facies including tuff, agglomerates, and ignimbrite (Du et al., 2020; Chen et al., 2020; this study; Fig. S1¹). Submarine sedimentary exhalative chert was also documented in Emeishan basaltic rocks in the basin (Liu et al., 1997), reflecting extensive Middle Permian submarine volcanogenic hydrothermal activity. The regional deep normal faults were likely generated by mantle plume-related uplift in the Emeishan large igneous province middle–outer zones (He et al., 2003; Xu et al., 2015) and were considered to be related to the syngenetic Au mineralization (Emsbo et al., 1999).

Petrography of the Qinglong–Nibao Volcanic-Sedimentary Rocks

The study area, the Qinglong–Nibao gold mining district in the northern part of the Youjiang basin, contains Middle to Upper Permian volcanic-sedimentary rocks, including bioclastic/cherty limestone, claystone, hyaloclastite

¹Supplemental Material. Text: Analytical Methods. Figure S1: Petrographic characteristics of volcanic facies including tuff layers, volcanic agglomerates and ignimbrites in the Middle-Permian carbonate platform, Qinglong area, Youjiang basin. Tables S1–S5. Please visit <https://doi.org/10.1130/GSAB.S.20277516> to access the supplemental material, and contact editing@geosociety.org with any questions.

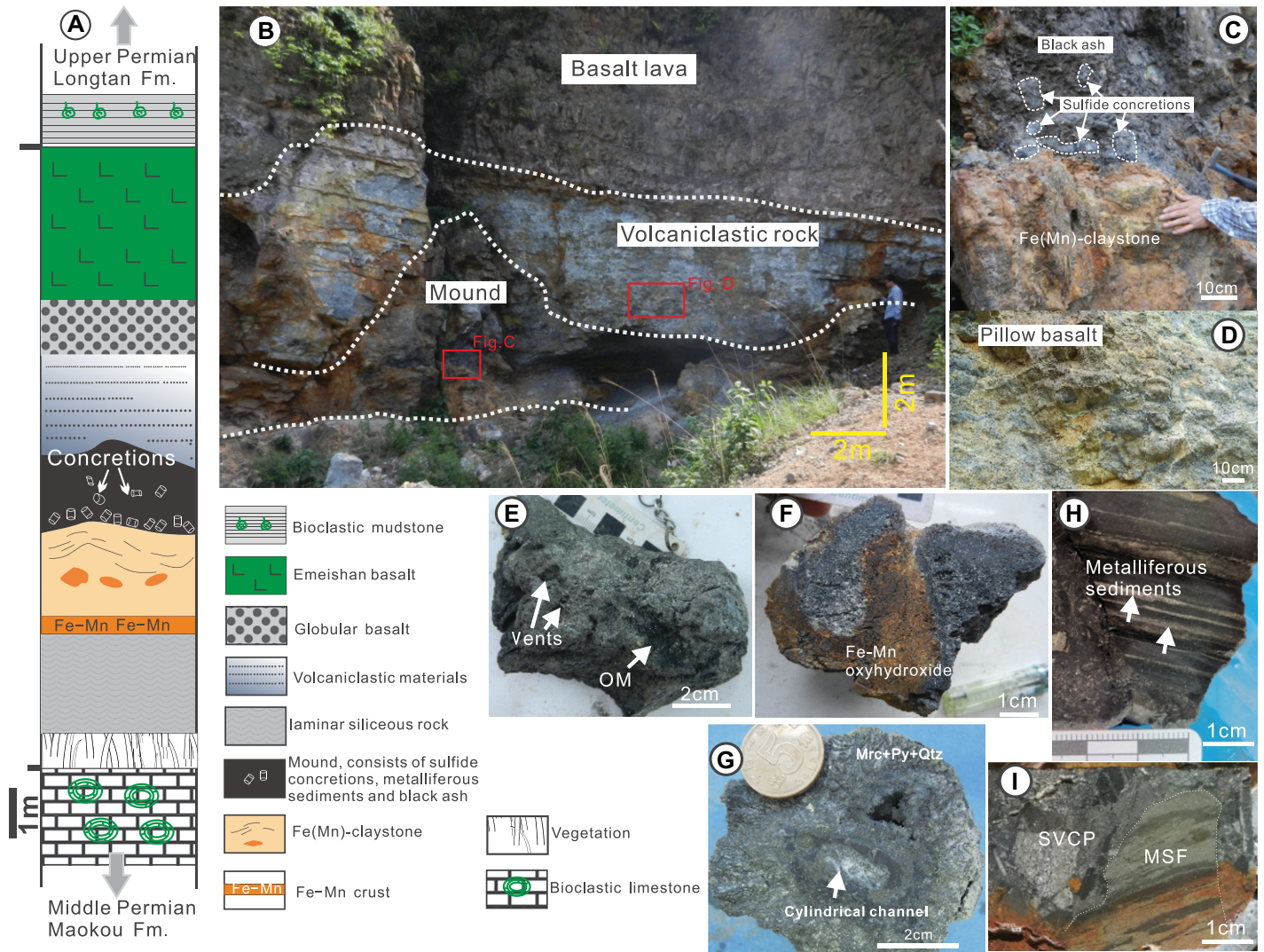


Figure 2. Middle–Upper Permian volcano-sedimentary sequences in the Qinglong district of the Youjiang basin are shown: (A) stratigraphic column of the Maokou Formation and Upper Longtan Formation; (B) outcrop profile of volcanic rocks shows the lithologic contact between the sulfide mound, volcaniclastic rocks, and basaltic lava; (C) occurrence of sulfide concretions in tuffaceous tuff and organic-rich claystone, which overlies the Fe(-Mn) claystone; (D) pillow basalt; (E–I) morphology, texture, and mineral assemblage of sulfide concretions and massive sulfide clasts. Abbreviations: OM—organic matter; Mrc—marcasite; Py—pyrite; Qtz—quartz; SVCP—scoria and volcanoclastic particles; MSF—massive sulfide fragment.

(tuff), and basalt (Fig. 2A). It is noteworthy that these volcanic-sedimentary rocks also host major Au-Sb-Hg ores (Chen et al., 2021), e.g., the Qinglong Sb(-Au) deposit (ca. 300 kt Sb resource; Chen et al., 2018) and the Nibao Au deposit (60 t at 2.74 g/t; Wei et al., 2020). The Au/Sb orebodies are stratabound and/or fault-controlled. The ore-related alteration mainly includes decarbonate, sulfide, argillic, dolomitic, and silicic rocks (Hu et al., 2017; Su et al., 2018; Chen et al., 2021). In contrast, there is no significant economic Au-Sb mineralization in unaltered volcanic-sedimentary rocks (Chen et al., 2018; Su et al., 2018; Li et al., 2021), even though these rocks contain some

pyrites and detectable gold (Wei et al., 2020; Chen et al., 2021).

Here, we examined a typical section of unaltered volcanic-sedimentary rock at Qinglong (Figs. 2A–2B). From bottom to top, seven layers were identified (Fig. 2A):

1: laminated chert (~1.6 m thick), which suggests submarine deep-water sedimentation.

2: thin, ferromanganese layer (~0.03 m thick), which suggests a cessation of terrigenous sediment supply (Fig. 2C). This is overlain by mafic submarine hyaloclastite deposit that formed metalliferous volcanic layers.

3: ferruginous claystone (2.4 m thick; Fig. 2C). Geochemical evidence suggests

that the claystone source is mafic tuffs from the early-stage Emeishan large igneous province volcanism (Du et al., 2020; Yan et al., 2020).

4: black sulfide mound (1–3 m thick; Fig. 2C) that consists of volcaniclastic particles, scoria, and sulfide concretions.

5: tuffaceous claystone beds (1–3 m thick), which are also widely distributed across the Youjiang basin. This bed yielded a zircon U–Pb age of ca. 262.5 Ma (Yan et al., 2020), which predates the Emeishan large igneous province subaerial eruptive phase.

6: pillow basalt (~1.0 m thick; Fig. 2D) that reflects submarine volcanism.

7: flood basalt (>10 m thick) that represents the later Emeishan large igneous province eruptive phases.

In particular, sulfide concretions were mainly found in the black mound (Figs. 2C and 2E–2F) and commonly formed chimney-like structures (with diameters of 8–15 cm; Fig. 2G) with sulfides deposited around a central conduit (Fig. 2G). These conduits likely represent hydrothermal fluid pathways. Around the central conduit, the chimney comprises massive pyrite in the core that is surrounded by radiating marcasite toward the margin (Fig. 2G). The chimney surface is semi-consolidated, highly porous (Fig. 2E), and composed of volcanoclastic materials and sulfides or locally coated with amorphous Fe-Mn oxyhydroxides (Fig. 2F). At Nibao (30 km away from Qinglong; Fig. 1B), sulfide (pyrite with minor sphalerite and chalcopyrite) laminae (Figs. 2H–2I) are underlain by the Middle Permian Maokou Formation and overlain by the Emeishan flood basalt, reflecting probable distal volcanogenic sulfide deposition.

SAMPLES AND ANALYTICAL METHODS

In this study, we identified the Emeishan large igneous province-related basalts, tuffs, sulfide concretions and metalliferous claystone along the Qinglong and Nibao sections in the northern Youjiang basin (Figs. 1A–1B). A total of 19 samples were fire assayed for the Au content. The mineralogy of the auriferous sulfides and sedimentary rocks was determined by a combination of scanning electron microscopy, electron probe micro-analysis (EPMA), and laser Raman spectrometry. Variations of trace element and sulfur isotope compositions of these auriferous sulfides (e.g., marcasite and pyrite) were determined with in situ laser ablation–inductively coupled plasma–mass spectrometry (LA-ICP-MS) and NanoSIMS analyses, respectively. Bulk-rock Pb isotope analysis for 13 basaltic rocks, auriferous sulfides, and sediments were carried out to constrain the metal source(s). Detailed analytical methods are given in the Supplemental Materials (see footnote one).

RESULTS AND DISCUSSION

Mineralogy

Sulfide concretions consist mainly of pyrite, marcasite, and sphalerite and minor barite, as well as amorphous silica and basaltic tuff groundmass (Figs. 3A–3D). Pyrite is the dominant mineral and shows various occurrences. The volcanoclastic sediments contain thin pyrite beds (termed “pinstripe pyrite”) dominated by

fine-grained anhedral pyrite with minor sphalerite (Fig. 2H). Unlike the pinstripe pyrite, massive pyrite occurs mostly as concretions and broken fragments and shows recrystallized coarse-grained euhedral texture, with some being fractured/replaced by marcasite (Fig. 3C). Small ilmenite inclusions commonly occur in the sulfides and amorphous silica (Figs. 3D–3E), which is also present in some basalt-hosted gold ores (Jiadi; Fig. 1B) with pre-ore igneous minerals (e.g., orthopyroxene, magnetite, ilmenite, and apatite; Li et al., 2021).

Native Gold

Petrographic observations show that the gold occurrence is dominated by tiny, discrete native gold grains (up to 10 μm) in the interstices of sulfides (pyrite and marcasite; Fig. 3H) or in the cavities of amorphous silica (Fig. 3G). Gold is also detected in these rocks by fire assay, with concentrations of 0.03–1.34 ppm (avg. 0.37 ppm, $n = 19$; Table S1; see footnote one). These auriferous rocks show no late alteration features (Fig. 2), although they still contain amorphous silica and barite (Figs. 3B and 3D). It is worth noting that such native gold occurrence contrasts markedly with much of the Carlin-type invisible, lattice-bound gold in the Youjiang basin (Su et al., 2018).

EPMA data reveal that single native gold grains contain 93.93–98.84 wt% Au (avg. 96.83 wt%), with trace Co, Ni, Ba, Zn, and Hg (Fig. 4A). The elemental assemblage is also similar to VMS-type elemental assemblages (Au, Fe, Pb, Zn, Cu, Hg, Co, Ni, Ag, Bi, Te, and Ba) in continental crustal environments (Iizasa et al., 2019; Fuchs et al., 2019) but markedly different from the Carlin-type elemental suite (Au, Sb, As, Hg, Tl, and Te; Su et al., 2018). Iizasa et al. (2019) described a gold-rich sulfide deposit in a submarine basaltic caldera of the Higashi-Aogashima hydrothermal field, which is situated in relatively thick continental crust in an intraoceanic arc setting. The gold-rich sulfide ores from Higashi-Aogashima also have similar native gold occurrence, texture, and sulfide concretion and metalliferous claystone as the Qinglong samples. In addition, EPMA mapping indicates that some gold grains coexist with tiny ilmenite and unidentified Cr-bearing oxide in the basaltic tuff (Fig. 4B).

In Situ Trace Elements and Sulfur Isotopes of Auriferous Sulfides

A total of 45 LA-ICP-MS trace element spot analyses were done on the pyrite ($n = 34$) and marcasite ($n = 11$) from the claystone and sulfide concretions (Table S2; see footnote one),

and the results were compared with the Carlin-type auriferous pyrite data from Qinglong (Chen et al., 2021; Fig. 5). The results reveal that these sulfides contain much lower Au (~ 0.21 ppm), Sb (~ 47 ppm), Cu (~ 60 ppm), and As (~ 436 ppm), but much higher Ti (mostly 9–778 ppm and up to 6000 ppm), Cr (up to 58 ppm), and Zr (up to 67 ppm) than the Carlin-type ore. In addition, our sulfide samples also have a considerably lower Co/Ni ratio (0.11–0.19) than those of Carlin-type and epithermal-type ores (Co/Ni > 1; Li et al., 2020). Such low sulfide Co/Ni ratio (<1) is commonly attributed to a sedimentary/diagenetic origin (Bralia et al., 1979), which suggests that these sulfides may have been deposited in a basalt-dominated seafloor environment during the Emeishan basalt eruption. This is also supported by the high Ti–Cr–Zr but low Co/Ni contents of our samples.

The sulfur isotope data are listed in Table S3 (see footnote one) and illustrated in Figure 6. Mineralogical studies show that the pyrite is commonly replaced by marcasite (Fig. 4C). These Fe-sulfides also coexist with organic matter in the sulfide concretions (Fig. 6A). The pyrite $\delta^{34}\text{S}$ values range from +11.8‰ to +15.7‰ (avg. +14.0‰; $n = 10$; Figs. 6B–6C), close to the Permian seawater $\delta^{34}\text{S}_{\text{sulfate}}$ value (+12‰ to +15‰; Claypool et al., 1980). This suggests that these pyrites were formed in a closed system with no major sulfur isotope fractionation during the sedimentation or diagenesis. These $\delta^{34}\text{S}$ values are characteristic of diagenetic pyrite formed by thermochemical reduction of seawater sulfate in a closed system (Rye and Ohmoto, 1974). Comparatively, marcasite has a much higher $\delta^{34}\text{S}$ value (+20.1‰ to +34.3‰, avg. +25.9‰, $n = 11$; Figs. 6D–6E). Experimental studies have documented that precipitation of pyrite and marcasite can occur rapidly (in a few hours) under hydrothermal temperature up to 220 °C (Qian et al., 2011). In a VMS environment, as high-temperature fluids (200–300 °C; Iizasa et al., 2019) percolated into seafloor sediments, the temperature at the vent fluid–seawater interface could increase episodically. Meanwhile, abundant H_2S is produced in sedimentary basins at 75–200 °C by thermochemical sulfate reduction (TSR; Ohmoto, 1972), which causes sulfur isotopic fractionation (10‰–25‰; Harrison and Thode, 1957; Seal, 2006) in the large closed system observed in our auriferous sulfide samples.

Lead Isotopes of Basaltic Rocks and Gold Ores

Lead isotope compositions in gold ores can be used to decipher the origin of precious metals (Kamenov et al., 2007). Thus, we measured

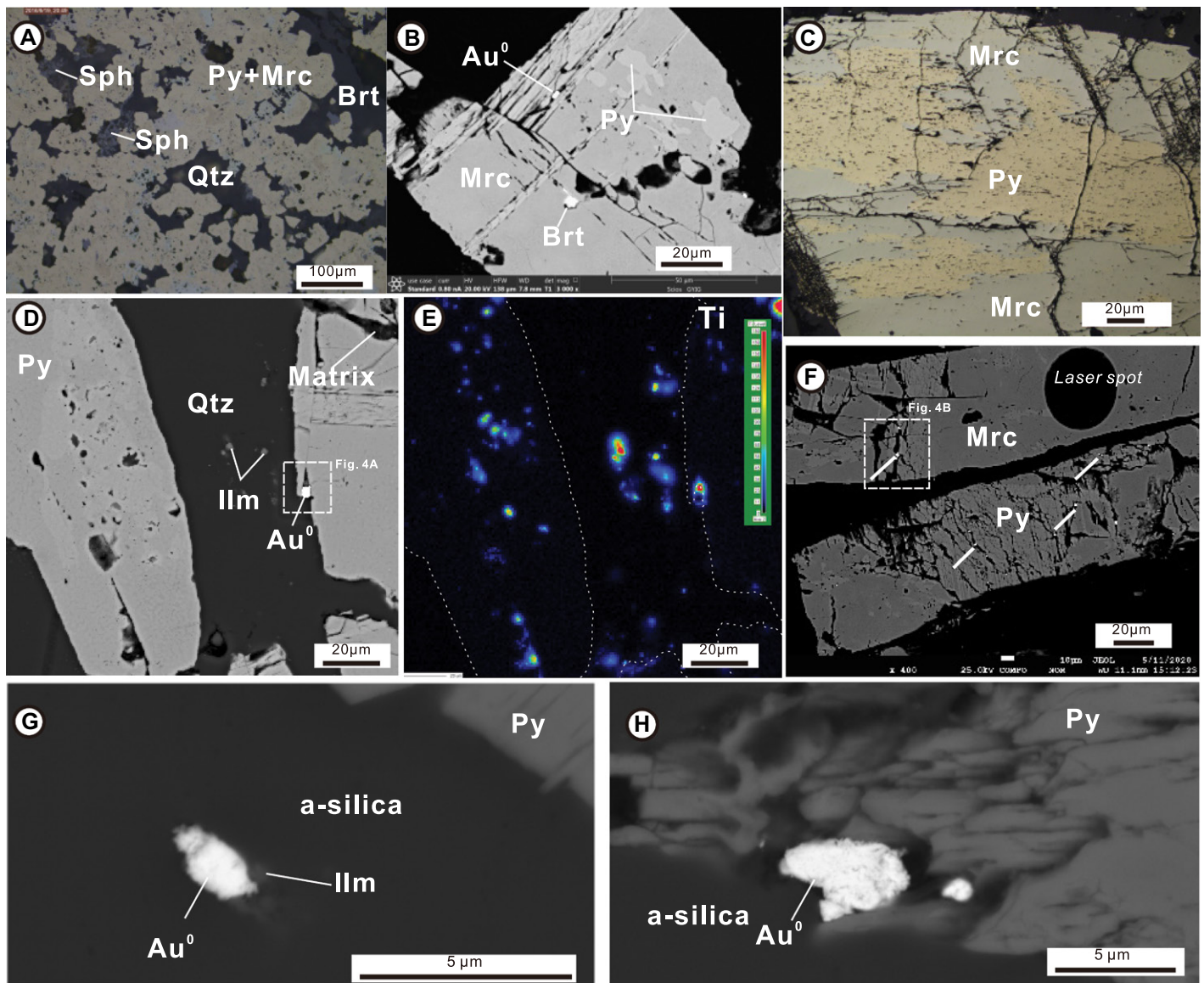


Figure 3. Representative photographs show sulfides (marcasite [Mrc], pyrite [Py], and sphalerite [Sph]), barite [Brt], ilmenite [Ilm] inclusions, and gold [Au⁰], as well as their relations in metalliferous sediments and sulfide concretions. (A) Py + Mrc coexists with Sph, Brt, and quartz (Qtz) in metalliferous sediments at Nibao mine. (B) Native gold and barite inclusions in microfracture of sulfides. (C) Py is replaced by Mrc. (D–E) Ilm inclusions in a-silica and sulfides; panel E shows an electron probe micro-analysis map. (F–H) Native gold with Ilm occurring as nano-particles (mostly <10 μm) in (G) a-silica and (H) pyrite.

the Pb isotope compositions of auriferous sulfide concretions ($n = 7$), claystone/tuff ($n = 3$), and pillow basalts ($n = 3$) from Qinglong. Meanwhile, comparing the published Pb isotope data (Zhang et al., 2006b) of the 259–263 Ma Lijiang picrite in the Emeishan large igneous province inner zone (Zhou et al., 2005) with those of the 251–255 Ma Shuicheng basalt (Lo et al., 2002; Liao et al., 2012) shows that the age-corrected ($t = 260$ Ma) Pb isotope ranges of the Qinglong samples are similar to those of the Lijiang picrites: $(^{206}\text{Pb}/^{204}\text{Pb})_t = 18.40$ – 19.35 , $(^{207}\text{Pb}/^{204}\text{Pb})_t = 15.60$ – 15.70 , and

$(^{208}\text{Pb}/^{204}\text{Pb})_t = 38.31$ – 40.10 , but different from those of the Shuicheng basalt (Liao, 2013; Fig. 7). The Qinglong data fall slightly above the picritic field in the $(^{206}\text{Pb}/^{204}\text{Pb})_t$ versus $(^{207}\text{Pb}/^{204}\text{Pb})_t$ plot and overlap or fall close to the picritic field in the $(^{206}\text{Pb}/^{204}\text{Pb})_t$ versus $(^{208}\text{Pb}/^{204}\text{Pb})_t$ plot. This suggests that the Qinglong samples may have had a Pb source similar to that of the picrites but may have undergone different Pb evolutionary processes (Figs. 7A–7B). In fact, the Lijiang picritic lavas represent the early-stage mantle-plume activity (ca. 259–263 Ma; Zhou et al., 2005), and the magmas may have undergone varying

degrees of fractionation and crustal assimilation (Zhang et al., 2006b; Tao et al., 2015). Zhang et al. (2006b) reported that the Lijiang picrite is interbedded with basalts and suggested that the latter was formed by fractionation of picritic magmas. This magmatic evolution may have also contributed to the Fe-Ti-V oxide mineralization, which is generally correlated to ferropicritic magmas (Hou et al., 2011, 2013; Bai et al., 2012). The similar Pb isotope compositions of the samples and the picritic lavas suggest that the local picritic magmas may have been the gold source. The presence of ilmenite and Cr-bearing oxide

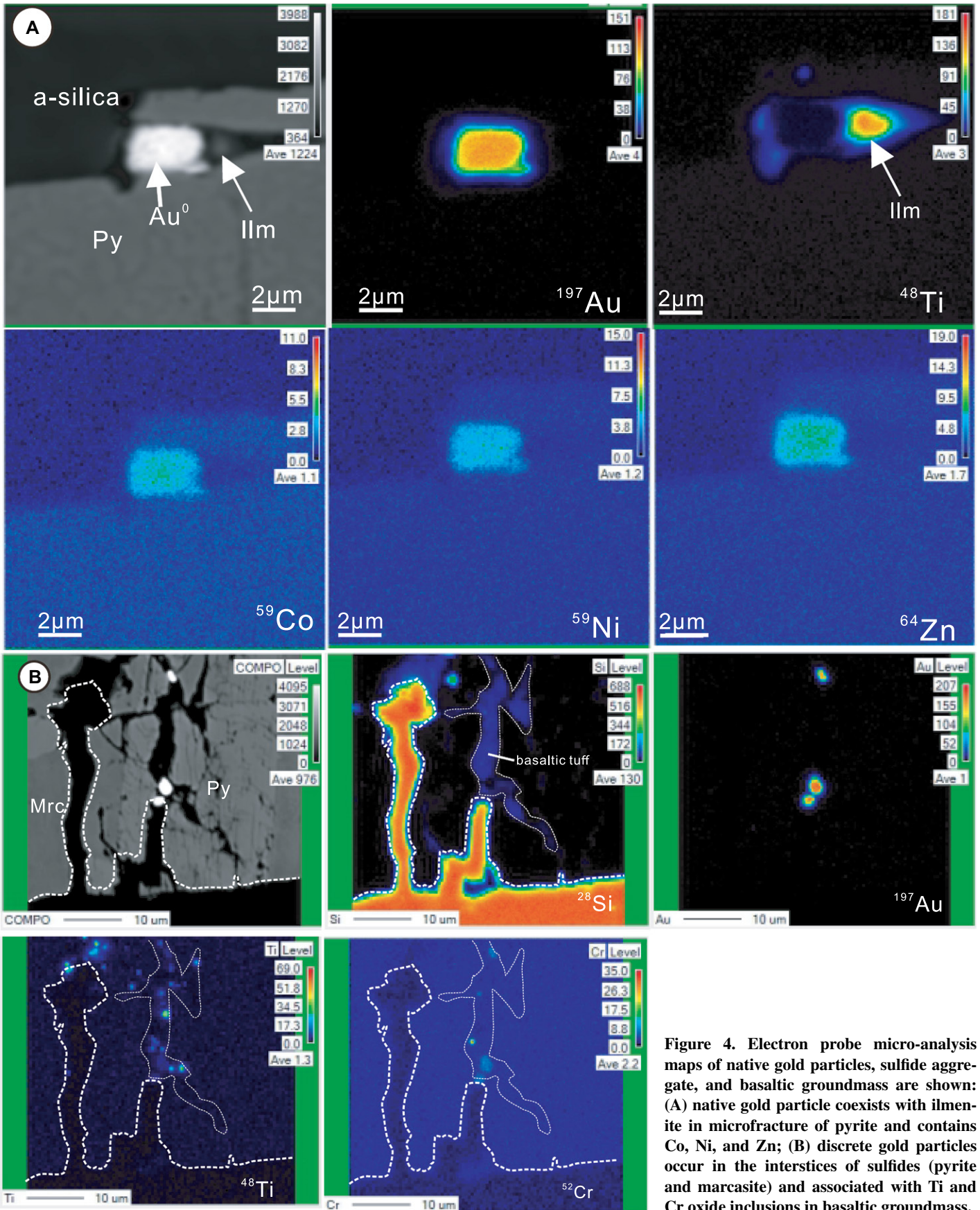


Figure 4. Electron probe micro-analysis maps of native gold particles, sulfide aggregate, and basaltic groundmass are shown: (A) native gold particle coexists with ilmenite in microfracture of pyrite and contains Co, Ni, and Zn; (B) discrete gold particles occur in the interstices of sulfides (pyrite and marcasite) and associated with Ti and Cr oxide inclusions in basaltic groundmass.

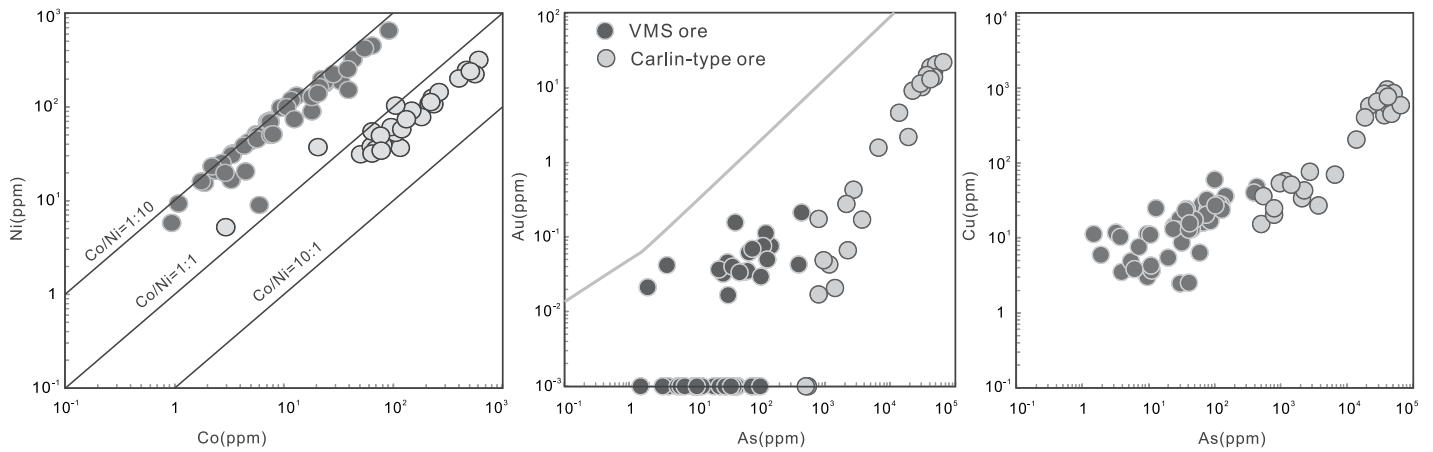


Figure 5. Trace element comparison between volcanogenic massive sulfides (VMS; pyrite and marcasite) and younger Carlin-type pyrites (data from Chen et al., 2021) show distinct geochemical features.

inclusions in the auriferous pyrite and amorphous silica (Figs. 3D and 4B) also supports a mafic-ultramafic magmatic origin (Xu et al., 2004). However, the more radiogenic Pb of these volcanic-sedimentary rocks (cf. picrites) implies mixing with a more radiogenic Pb (high $^{207}\text{Pb}/^{204}\text{Pb}$) source, possibly the Devonian–Permian basinal carbonates with elevated $^{207}\text{Pb}/^{204}\text{Pb}$ ratios (up to 16,000; Zhou et al., 2014).

Gold Enrichment in Mantle Plume and Gold Source in the Youjiang Basin

Origin and Deposition of Native Gold

Gold enrichment in the mantle source has been proposed to be key for giant gold mineralization

(e.g., epithermal Au-Ag deposits; Tassara et al., 2017). It is reported that mantle plumes may have brought deep-seated, Au-mineralized spinel lherzolite xenoliths to the surface (Wilshire and Shervais, 1975; Zhang et al., 2006a). In fact, siderophile elements and platinum group elements (PGEs) were suggested to have derived mainly from mantle plumes and formed many important magmatic Fe-Ti-V oxide, Ni-Cu-PEG sulfide, and Cr deposits in the Emeishan large igneous provinces (Ernst, 2014).

At Qinglong, auriferous sulfides (pyrite and marcasite) have much higher siderophile element (e.g., Ti, Cr, and Zr) contents, which is consistent with these elements being enriched in mantle plumes (Boyle, 1979; Burke et al.,

2008; Hawkesworth and Schersten, 2007; Bierlein and Pisarevsky, 2008). Native gold particles coexist with ilmenite and minor unidentified Cr oxide inclusions in pyrite and amorphous silica, which further supports gold transport from the mantle plume into the VMS system. Plume-subduction interaction with subcontinental lithospheric mantle could have induced Au-rich magmas and produced a transient Au storage zone in the plume-mantle boundary (Tassara et al., 2017; Fig. 8A). The Au-bearing melt may have ascended with the rising plume from the transient storage zone when connected to the overlying crust by deep faults (Griffin et al., 2013; Fig. 8A). Upon ascent, the melt may have decompressed, with the gold forming

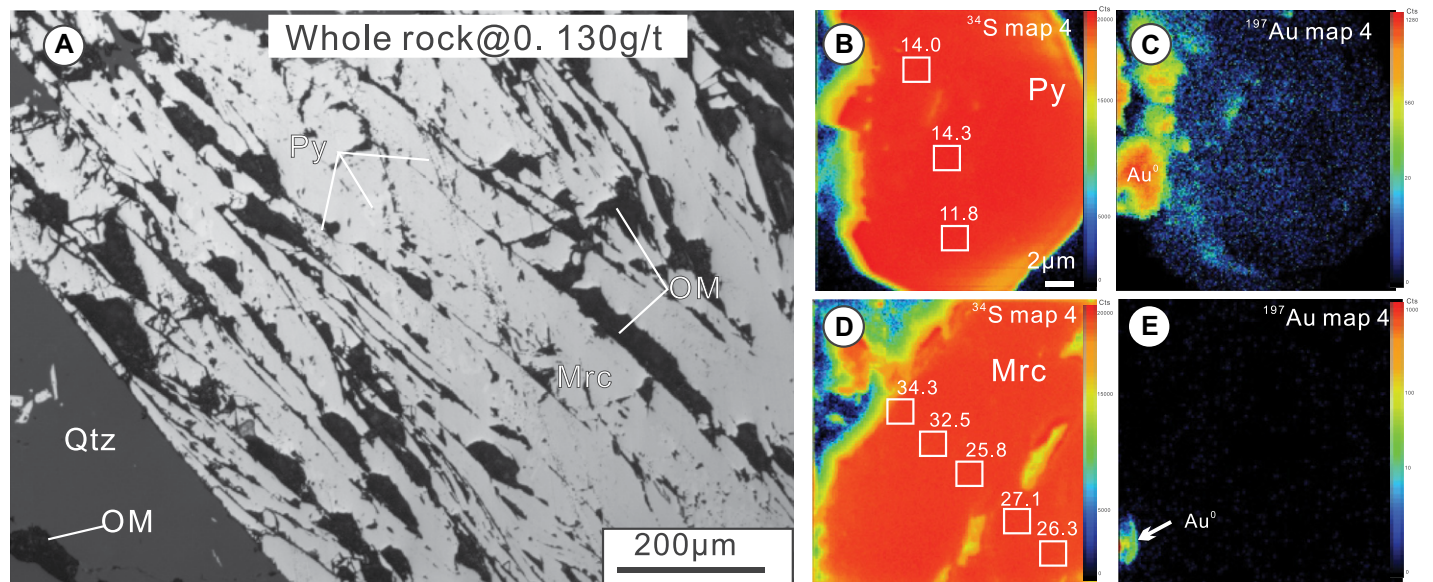


Figure 6. Organic matter coexists with pyrite and marcasite in sulfide concretions: (A) sulfate reacts with organic matter via thermochemical sulfate reduction (TSR), causing major sulfur isotopic fractionation; nanoSIMS element maps of (B and D) ^{34}S and (C and E) ^{197}Au show $\delta^{34}\text{S}$ variation of pyrite and marcasite (from Chen et al., 2020).

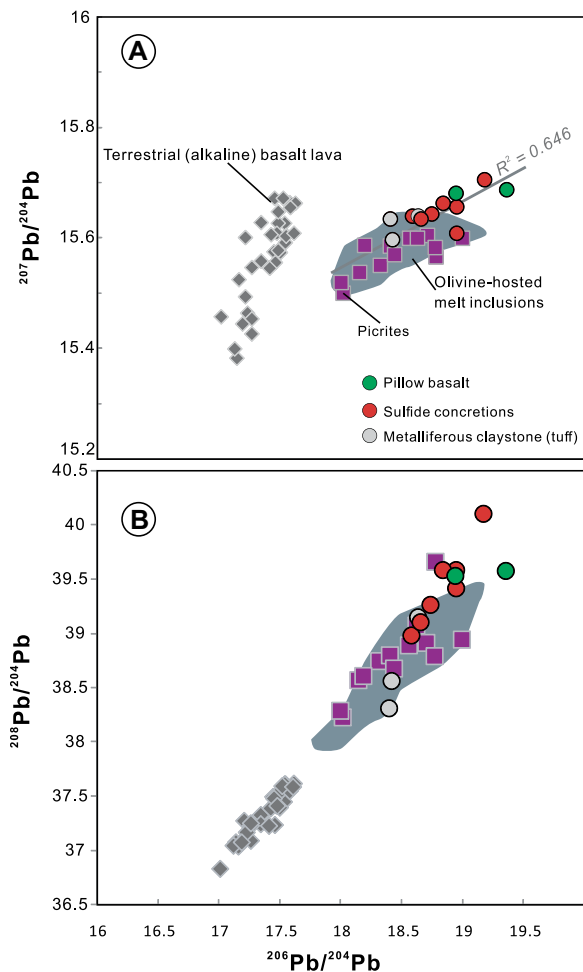


Figure 7. (A) $^{206}\text{Pb}/^{204}\text{Pb}_{(t)}$ versus $^{207}\text{Pb}/^{204}\text{Pb}_{(t)}$ and (B) $^{206}\text{Pb}/^{204}\text{Pb}_{(t)}$ versus $^{208}\text{Pb}/^{204}\text{Pb}_{(t)}$ are plotted for auriferous volcanic rocks from the Qinglong section of the Youjiang basin. Lead isotope data source: picrite is from Zhang et al. (2006b); olivine-hosted melt inclusions are from Ren et al. (2017); Guizhou terrestrial basaltic lava is from Liao (2013). Age-corrected ($t = 260$ Ma) Pb isotope ratios of the auriferous volcanic rocks define a linear array comparable to the picrite field.

blebs in the magmatic volatiles, as reported in the basanite glass of the early submarine volcanic phase in the Kilauea volcano, Hawaii (Sisson, 2003). The native gold grains from Qinglong also contain hydrothermal markers such as Co, Ba, Zn, and Ni (Fig. 4A), which suggests Au remobilization and reprecipitation in a VMS environment. Consistently, mineral assemblage (pyrite, marcasite, barite, and sphalerite) in the volcanoclastic beds at Qinglong is VMS-like, and these sulfides have lower Co/Ni ratios (<0.2). Our sulfide chimney surface sample is porous, fragmented, and has Fe-Mn oxyhydroxide (Figs. 2E–2F), similar to the Higashi-Aogashima auriferous sulfide concretions (Iizasa et al., 2019). The explosive volcanic facies (including tuff, agglomerate, and ignimbrite) at Qinglong (Du et al., 2020) also implies a concealed caldera beneath the subaerial basaltic lavas. In addition, the lack of late alteration in the volcanic-sedimentary sequences (e.g., Carlin-type silicification and decarbonization) rules out that these gold grains were deposited in the later Carlin-type Au mineralization (ca. 140 Ma; Chen et al., 2019).

The Emeishan picrites were likely formed from more primitive magmas and are less contaminated by crust than the basalts (Zhang et al., 2006b, 2008; Yao et al., 2019). Based on the presence of native Cu and the absence of sulfide in the Emeishan large igneous province picrites (Zhang et al., 2006a), the primary magma may have been strongly S-undersaturated. Thus, it is unlikely that gold was released from sulfides during the progressive sulfide resorption. As alkalic melts derived from mantle plumes could increase the Au solubility (Sisson, 2003), plume-derived (sub-)alkalic melts may have increased the overall magma Au content (Zhu et al., 2020). Evidence of vapor-assisted metal transport and deposition implies that gold was transported and precipitated from a vapor phase in mafic plutonic systems (Li and Boudreau, 2019, and references therein). As gold-rich magmatic vapor (from plume degassing) ascended to the cooler shallow crust, the metals may have precipitated via cooling and/or redox change that destabilized the metal complexes (Christie et al., 1986). Under these conditions, as the auriferous magmatic gases ascended toward the seafloor (e.g.,

carbonate platform at Qinglong; Fig. 8B), gold may have initially precipitated in high-temperature boiling fluid due to pressure drop and then transported particulates into the low-temperature vents (Gartman et al., 2018), forming the native gold particles in our sulfide concretion and sediment samples. Meanwhile, base metals (e.g., Fe, Zn, Co, Ba, and Hg), combined with reduced sulfur (TSR from seawater sulfates), likely caused sulfide deposition. The elevated magmatic volatile contents may have also produced the abundant volcanoclastics (including tuff and breccias) on the Middle Permian seafloor (Fig. 8B).

Implications for Large-Scale Au Mineralization in the Youjiang Basin

The native gold and associated sulfide (pyrite and marcasite) geochemistry are markedly different from the younger Carlin-type gold mineralization in the Youjiang basin, which provides an alternative view regarding the gold source in the basin. In fact, rare native gold grains in younger Carlin-type ores from the Youjiang basin were also reported by previous studies (Su et al., 2018; Li et al., 2020). These gold grains are 1–6 μm large and commonly present in the core of zoned auriferous pyrite (Figs. 9E–9F; Li et al., 2020). These pyrite cores are of diagenetic origin, as supported by the lower ore or pathfinder element (e.g., Au, Sb, As, and Hg) contents and wider $\delta^{34}\text{S}$ range than the hydrothermal pyrite rim (Xie et al., 2018; Li et al., 2020). It is proposed that the native gold grains in the Early Cretaceous (ca. 140 Ma) Carlin-type ores were inherited from the Permian auriferous basaltic rocks.

In the Youjiang basin, the pyrite rims from the Carlin-type Au ores (Shuiyindong, Taipingdong, Nayang, Getang, and Lianhuashan) have near-zero $\delta^{34}\text{S}$ values (mostly -3‰ to $+3\text{‰}$; Chen et al., 2021), and the sulfur was proposed to be derived from the Emeishan basaltic rocks (Hu et al., 2018) or a deep magmatic source (Xie et al., 2018; Chen et al., 2021). In addition, the ore-related hydrothermal zircon $\delta^{18}\text{O}_{\text{VSMOW}}$ values also show that the ore-forming fluids have had a magmatic origin (Zhu et al., 2020). However, apart from the Emeishan basalts, there are no other magmatic events reported in the Au/Sb mining districts in the basin. Hence, the magmatic sulfur was likely provided by the Emeishan basalts, although more work is needed to confirm that.

At Nibao (Fig. 1B), the auriferous zoned pyrite and interpreted VMS sulfide fragments were cemented by hydrothermal quartz (Fig. 9A). LA-ICP-MS trace element analysis of the zoned pyrite shows the presence of As-rich mantle, which probably formed via transformation and recrystallization of diagenetic

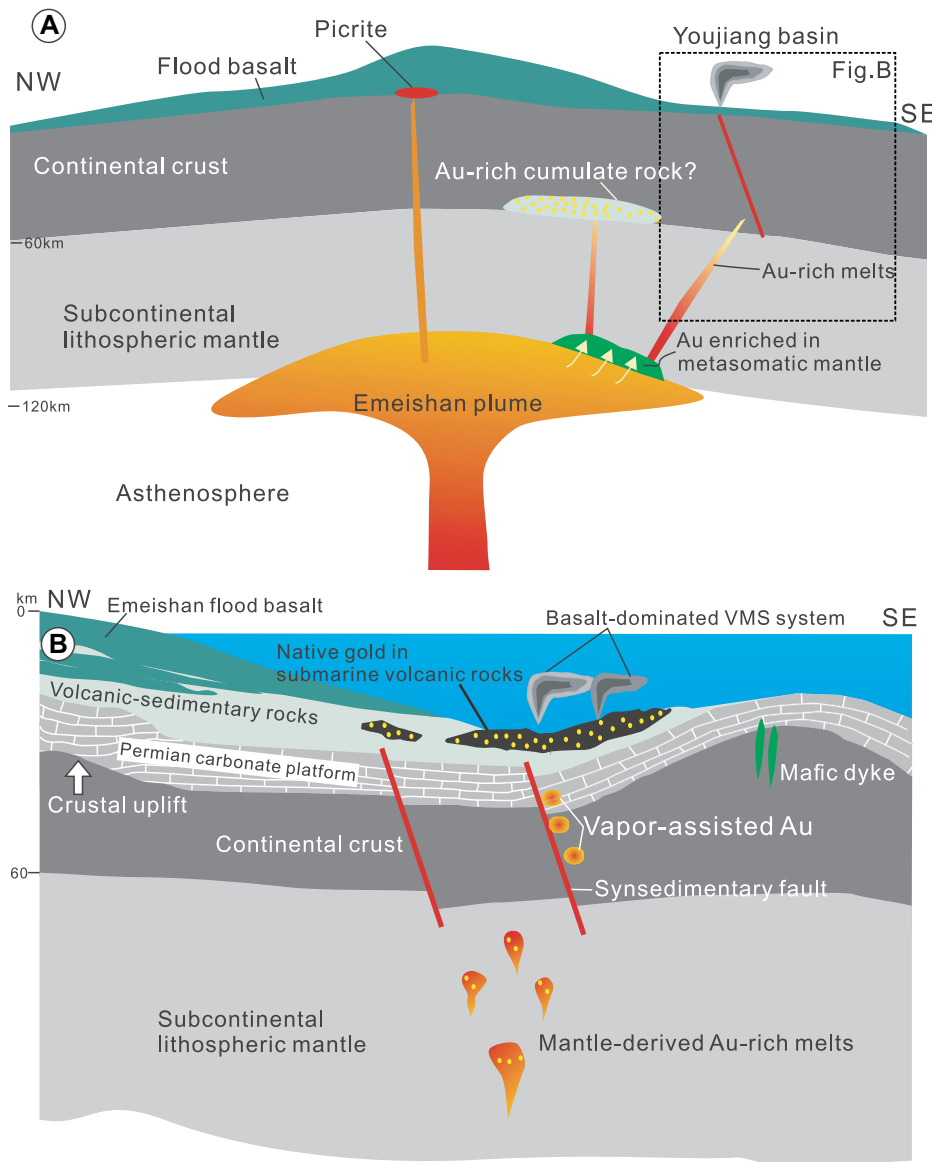


Figure 8. Schematic model shows mantle-sourced gold transport to the volcanogenic massive sulfide (VMS) system. (A) Plume interaction with the subcontinental lithospheric mantle induced gold enrichment in the metasomatized mantle (Tassara et al., 2017). Alternatively, metasomatism may have also generated an Au-rich juvenile lower crust that evolved from the primary plume-derived magmas (Zhu et al., 2020). (B) Deposition of mantle-sourced Au in VMS system; deep-mantle upwelling brought the Au-rich melts into the continental crust and transformed them to gold captured in magmatic volatiles. As the auriferous volatiles ascended toward the seafloor, precipitation of gold and sulfides occurred along with the formation of abundant volcanoclastics, including tuff and breccias. (A) The mantle-plume model is modified from Yao et al. (2019) and (B) the sedimentary model of the Youjiang basin is from Du et al. (2020).

pyrite grains (Fig. 9B). This replacement process is also reflected in the LA-ICP-MS time-resolved signal spectra of the different pyrite zones from Qinglong, which show that the trace element distributions are heterogeneous in the core (upward-convex signal curves; Fig. 9C) but homogeneous in the mantle (smooth, flat

signal curves; Fig. 9D). The replacement may have occurred when an external fluid (e.g., metamorphic fluid for the younger Carlin-type gold mineralization; Su et al., 2009) came into contact with pre-existing auriferous sulfides (e.g., pyrite and marcasite at Qinglong), remobilizing gold and other trace elements from the pyrite crystal

lattice, and then reprecipitated them in the pyrite replacement zone(s) (Wu et al., 2019). All of the above evidence implies that the syngenetic gold mantle-sourced in pre-existing diagenetic pyrite can be enriched in hydrothermal replacement zones via dissolution and reprecipitation.

CONCLUSIONS

Our study indicates that native gold particles found in unaltered submarine basaltic rocks were derived from the mantle during previous degassing of the Emeishan plume activity and accumulated in a submarine VMS system. Alternatively, in the younger Carlin-type mineralization, the auriferous basaltic rocks may have been pre-enriched with gold. Quantitative assessment is needed to determine whether sufficient gold could be supplied by the Emeishan plume to produce the regional gold mineralization. Our findings provide direct evidence of gold enrichment during the Emeishan plume activity and also an alternative view on the gold source in the Youjiang basin.

ACKNOWLEDGMENTS

We are grateful to Wen-Bo Li and an anonymous reviewer for their very insightful and constructive reviews. We thank Xiang Li for laboratory assistance. This research was supported by the National Natural Science Foundation of China (41902085), the Open Research Foundation of the State Key Laboratory of Ore Deposit Geochemistry (IGCAS; 201905, 202210), the Breeding Project of the Guizhou University (202007), and the Natural Science Research Funding (Special Project) in the Guizhou University (202228).

REFERENCES CITED

- Ali, J.R., Thompson, G.M., Zhou, M.F., and Song, X.Y., 2005, Emeishan large igneous province, SW China: *Lithos*, v. 79, p. 475–489, <https://doi.org/10.1016/j.lithos.2004.09.013>.
- Bai, Z.J., Zhong, H., Naldrett, A.J., Zhu, W.G., and Xu, G.W., 2012, Whole-rock and mineral composition constraints on the genesis of the giant Hongge Fe-Ti-V oxide deposit in the Emeishan large igneous province, Southwest China: *Economic Geology*, v. 107, p. 507–524, <https://doi.org/10.2113/econgeo.107.3.507>.
- Bierlein, F.P., and Pisarevsky, S., 2008, Plume-related oceanic plateaus as a potential source of gold mineralization: *Economic Geology*, v. 103, p. 425–430, <https://doi.org/10.2113/gsecongeo.103.2.425>.
- Boyle, R.W., 1979, The geochemistry of gold and its deposits: *Geological Survey of Canada Bulletin*, v. 280, p. 1–584, <https://doi.org/10.4095/105577>.
- Bralia, A., Sabatini, G., and Troja, F., 1979, A reevaluation of the Co/Ni ratio in pyrite as geochemical tool in ore genesis problems: *Mineralium Deposita*, v. 14, p. 353–374, <https://doi.org/10.1007/BF00206365>.
- Brandon, A.D., and Walker, R.J., 2005, The debate over core-mantle interaction: *Earth and Planetary Science Letters*, v. 232, p. 211–225, <https://doi.org/10.1016/j.epsl.2005.01.034>.
- Burke, K., Steinberger, B., Torsvik, T.H., and Smethurst, M.A., 2008, Plume generation zones at the margins of large low shear velocity provinces on the core-mantle boundary: *Earth and Planetary Science Letters*, v. 265, p. 49–60, <https://doi.org/10.1016/j.epsl.2007.09.042>.
- Chen, J., Yang, R.D., Du, L.J., Zheng, L.L., Gao, J.B., Lai, C.K., Wei, H.R., and Yuan, M.G., 2018, *Mineralogy*,

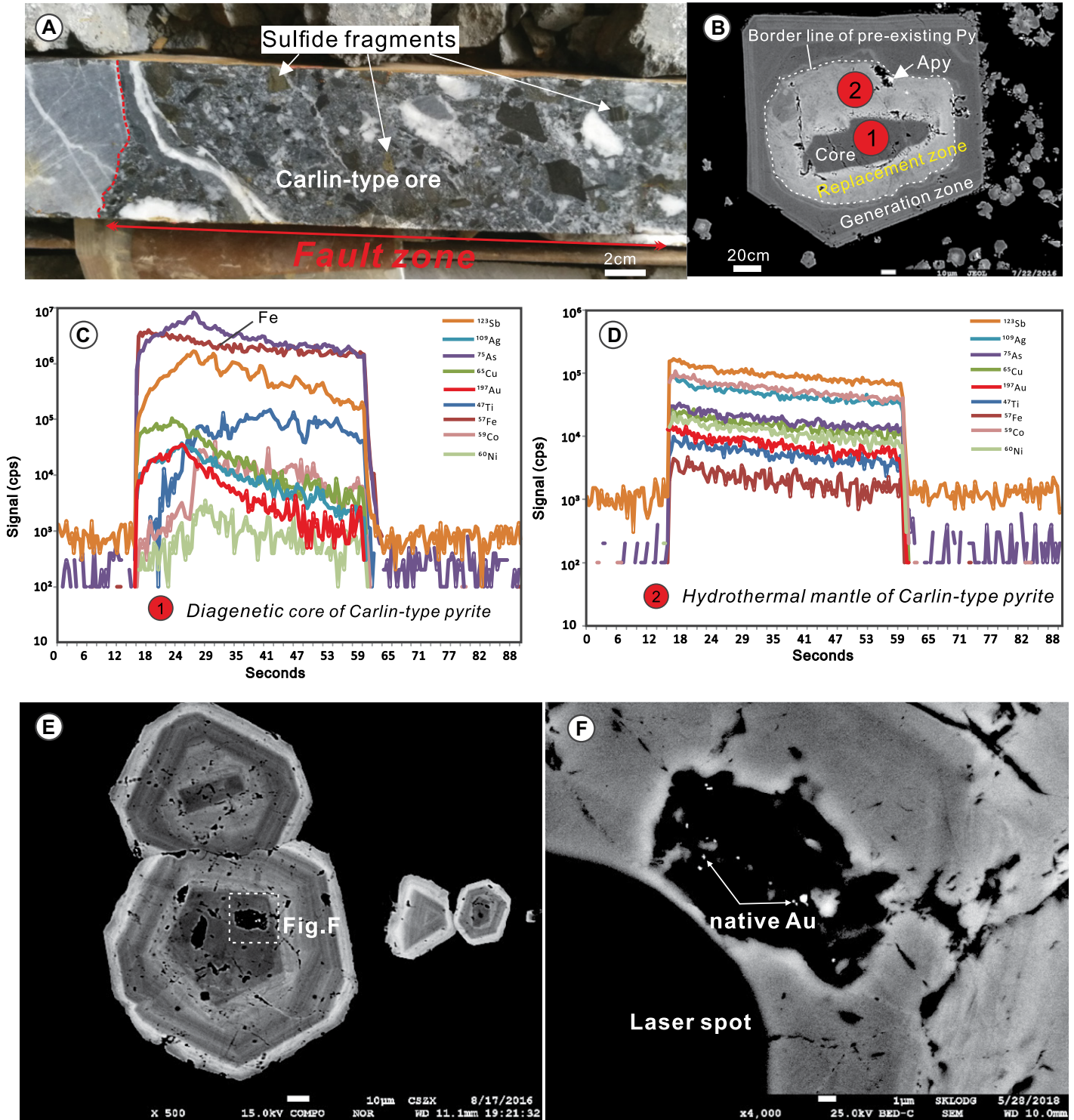


Figure 9. Schematic diagram shows genetic relations between Middle Permian syngenetic gold (ca. 260 Ma) and younger Carlin-type gold (ca. 140 Ma) ores. (A) Auriferous pyrite and volcanogenic massive sulfide (VMS) fragments are cemented by hydrothermal quartz at Nibao; (B) arsenic-rich pyrite mantle formed via dissolution and recrystallization of pre-existing pyrite; (C–D) laser ablation–inductively coupled plasma–mass spectrometry (LA–ICP–MS) time-resolved signal spectra for different pyrite zones at Qinglong show that trace element distributions are homogeneous in the pyrite mantle but heterogeneous in the core; (E–F) syngenetic gold grains were inherited in the Carlin-type pyrite at Shuiyindong (Li et al., 2020).

- geochemistry and fluid inclusions of the Qinglong Sb-(Au) deposit, Youjiang basin (Guizhou, SW China): *Ore Geology Reviews*, v. 92, p. 1–18, <https://doi.org/10.1016/j.oregeorev.2017.11.009>.
- Chen, J., Huang, Z.L., Yang, R.D., Du, L.J., Su, W.C., Zheng, L.L., and Ye, L., 2020, Discovery of SEDEX gold in the Youjiang basin, SW China: Implications for a new type Au mineralization: *Chinese Science Bulletin*, v. 65, p. 1486–1495, <https://doi.org/10.1360/TB-2019-0837>.
- Chen, J., Huang, Z.L., Yang, R.D., Du, L.J., and Liao, M.Y., 2021, Gold and antimony metallogenic relations and ore-forming process of Qinglong Sb(Au) deposit in Youjiang basin, SW China: Sulfide trace elements and sulfur isotopes: *Geoscience Frontiers*, v. 12, p. 605–623, <https://doi.org/10.1016/j.gsf.2020.08.010>.
- Chen, M.H., Bagas, L., Liao, X., Zhang, Z.Q., and Li, Q.L., 2019, Hydrothermal apatite SIMS Th–Pb dating: Constraints on the timing of low-temperature hydrothermal Au deposits in Nibao, SW China: *Lithos*, v. 324, p. 418–428, <https://doi.org/10.1016/j.lithos.2018.11.018>.
- Christie, D.M., Carmichael, I.S.E., and Langmuir, C.H., 1986, Oxidation states of mid-ocean ridge basalt glasses: *Earth and Planetary Science Letters*, v. 79, p. 397–411, [https://doi.org/10.1016/0012-821X\(86\)90195-0](https://doi.org/10.1016/0012-821X(86)90195-0).
- Claypool, G.E., Holser, W.T., Kaplan, I.R., Sakai, H., and Zak, I., 1980, The age curves of sulfur and oxygen in marine sulfate and their initial interpretation: *Chemical Geology*, v. 28, p. 199–260, [https://doi.org/10.1016/0009-2541\(80\)90047-9](https://doi.org/10.1016/0009-2541(80)90047-9).
- Cline, J.S., Hofstra, A.H., Muntean, J.L., Tosdal, R.M., and Hickey, K.A., 2005, Carlin-type gold deposits in Nevada, USA: Critical geologic characteristics and viable models: *Economic Geology 100th Anniversary Volume*, p. 451–484.
- Du, L.J., Chen, J., Yang, R.D., Huang, Z.L., Zheng, L.L., Gao, J.B., and Wei, H.R., 2020, Hydrothermal-volcanic sedimentary and mineralization of the Dachang Layer in the Middle–Late Permian, Qinglong, southwestern Guizhou [in Chinese with English abstract]: *Dizhi Lunping*, v. 66, p. 440–456.
- Emsbo, F., Hutchinson, R.W., Hofstra, A.H., Volk, J.A., Bettles, K.H., Baschuk, G.J., and Johnson, C.A., 1999, Syngenetic Au on the Carlin trend: Implications for Carlin-type deposits: *Geology*, v. 27, p. 59–62, [https://doi.org/10.1130/0091-7613\(1999\)027<0059:SAOTCT>2.3.CO;2](https://doi.org/10.1130/0091-7613(1999)027<0059:SAOTCT>2.3.CO;2).
- Ernst, R.E., 2014, *Large Igneous Provinces*: Cambridge, UK, Cambridge University Press, p. 1–653, <https://doi.org/10.1017/CBO9781139025300>.
- Fuchs, S., Hannington, M.D., and Petersen, S., 2019, Diving gold in seafloor polymetallic massive sulfide systems: *Mineralium Deposita*, v. 54, p. 789–820, <https://doi.org/10.1007/s00126-019-00895-3>.
- Gao, J.B., Yang, R.D., Xu, H., Zhang, X., Feng, K.N., and Zheng, L.L., 2018, Genesis of Permian sedimentary manganese deposits in Zunyi, Guizhou Province, SW China: Constraints from geology and elemental geochemistry: *Journal of Geochemical Exploration*, v. 192, p. 142–154, <https://doi.org/10.1016/j.jgeexplo.2018.06.012>.
- Gartman, A., Hannington, M., Jamieson, J.W., Peterkin, B., Garbe-Schonberg, D., Findlay, A.J., Fuchs, S., and Kwasnitschka, T., 2018, Boiling-induced formation of colloidal gold in black smoker hydrothermal fluids: *Geology*, v. 46, p. 39–42, <https://doi.org/10.1130/G39492.1>.
- Griffin, W.L., Begg, G.C., and O'Reilly, S.Y., 2013, Continental-root control on the genesis of magmatic ore deposits: *Nature Geoscience*, v. 6, p. 905–910, <https://doi.org/10.1038/ngeo1954>.
- Harrison, A.G., and Thode, H.G., 1957, The kinetic isotope effect in the chemical reduction of sulphate: *Transactions of the Faraday Society*, v. 53, p. 1648–1651, <https://doi.org/10.1039/tf9575301648>.
- Hawkesworth, C., and Schersten, A., 2007, Mantle plumes and geochemistry: *Chemical Geology*, v. 241, p. 319–331, <https://doi.org/10.1016/j.chemgeo.2007.01.018>.
- He, B., Xu, Y.G., Chung, S.L., Xiao, L., and Wang, Y.M., 2003, Sedimentary evidence for a rapid, kilometer-scale crustal doming prior to the eruption of the Emeishan flood basalts: *Earth and Planetary Science Letters*, v. 213, p. 391–405, [https://doi.org/10.1016/S0012-821X\(03\)00323-6](https://doi.org/10.1016/S0012-821X(03)00323-6).
- Hou, T., Zhang, Z.C., Ye, X.R., Encarnacion, J., and Reichow, M.K., 2011, Noble gas isotopic systematics of Fe–Ti–V oxide ore-related mafic-ultramafic layered intrusions in the Panxi area, China, the role of recycled oceanic crust in their petrogenesis: *Geochimica et Cosmochimica Acta*, v. 75, p. 6727–6741, <https://doi.org/10.1016/j.gca.2011.09.003>.
- Hou, T., Zhang, Z.C., Encarnacion, J., Santosh, M., and Sun, Y.L., 2013, The role recycled oceanic crust in magmatism and metallogenesis, Os–Sr–Nd isotopes, U–Pb geochronology and geochemistry of picritic dykes in the Panzhihua giant Fe–Ti oxide deposit, central Emeishan large igneous province: *Contributions to Mineralogy and Petrology*, v. 165, p. 805–822, <https://doi.org/10.1007/s00410-012-0836-3>.
- Hu, R.Z., Fu, S.L., Huang, Y., Zhou, M.F., Fu, S.H., Zhao, C.H., Wang, Y.J., Bi, X.W., and Xiao, J.F., 2017, The giant South China Mesozoic low-temperature metallogenic domain: Reviews and a new geodynamic model: *Journal of Asian Earth Sciences*, v. 137, p. 9–34, <https://doi.org/10.1016/j.jseaes.2016.10.016>.
- Hu, X.L., Zeng, G.P., Zhang, Z.J., Li, W.T., Liu, W.H., Gong, Y.Z., and Yao, S.Z., 2018, Gold mineralization associated with Emeishan basaltic rocks: Mineralogical, geochemical, and isotopic evidences from the Lianhuashan ore field, southwestern Guizhou Province, China: *Ore Geology Reviews*, v. 95, p. 604–619, <https://doi.org/10.1016/j.oregeorev.2018.03.016>.
- Huang, H., Cawood, P.A., Hou, M.C., Yang, J.H., Ni, S.J., Du, Y.S., Yan, Z.K., and Wang, J., 2016, Silicic ash beds bracket Emeishan Large Igneous Province to <1 m.y. at ~260 Ma: *Lithos*, v. 264, p. 17–27, <https://doi.org/10.1016/j.lithos.2016.08.013>.
- Iizasa, K., Asada, A., Mizuno, K., Katase, F., Lee, S., Kojima, M., and Ogawa, N., 2019, Native gold and gold-rich sulfide deposits in a submarine basaltic caldera, Higashi-Aogashima hydrothermal field, Izu-Ogasawara frontal arc, Japan: *Mineralium Deposita*, v. 54, p. 117–132, <https://doi.org/10.1007/s00126-018-0808-2>.
- Jerram, D.A., Widdowson, M., Wignall, P.B., Sun, Y.D., Lai, X.L., Bond, D.P.G., and Torsvik, T.H., 2016, Submarine palaeoenvironments during Emeishan flood basalt volcanism, SW China: Implications for plume–lithosphere interaction during the Capitanian, Middle Permian ('end Guadalupian') extinction event: *Palaeogeography, Palaeoclimatology, Palaeoecology*, v. 441, p. 65–73, <https://doi.org/10.1016/j.palaeo.2015.06.009>.
- Kamenov, G.D., Saunders, J.A., Hames, W.E., and Unger, D.L., 2007, Mafic magmas as sources for gold in middle Miocene epithermal deposits of the northern great basin, United States: Evidence from Pb isotope compositions of native gold: *Economic Geology*, v. 102, p. 1191–1195, <https://doi.org/10.2113/gsecongeo.102.7.1191>.
- Keays, R.R., and Scott, R.B., 1976, Precious metals in ocean-ridge basalts: implications for basalts as source rocks for gold mineralization: *Economic Geology*, v. 71, p. 705–720, <https://doi.org/10.2113/gsecongeo.71.4.705>.
- Li, J.H., Wu, P., Xie, Z.J., Liu, J.Z., Zhang, S.J., Song, W.F., Zhang, B.Q., Li, S.T., Xu, L.Y., and Zheng, L.L., 2021, Alteration and paragenesis of the basalt-hosted Au deposits, southwestern Guizhou Province, China: Implications for ore genesis and exploration: *Ore Geology Reviews*, v. 131, <https://doi.org/10.1016/j.oregeorev.2021.104034>.
- Li, J.X., Hu, R.Z., Zhao, C.H., Zhu, J.J., Huang, Y., Gao, W., Li, J.W., and Zhuo, Y.Z., 2020, Sulfur isotope and trace element compositions of pyrite determined by NanoSIMS and LA-ICP-MS: New constraints on the genesis of the Shuiyindong Carlin-like gold deposit in SW China: *Mineralium Deposita*, v. 55, p. 1279–1298, <https://doi.org/10.1007/s00126-019-00929-w>.
- Li, P., and Boudreau, A.E., 2019, Vapor transport of silver and gold in basaltic lava flows: *Geology*, v. 47, p. 877–880, <https://doi.org/10.1130/G46407.1>.
- Liao, B.L., 2013, Study of petrology and geochemistry of the Permian alkaline basalt in Guizhou Province [Ph.D. dissertation; in Chinese with English abstract]: Beijing, China University of Geosciences, p. 1–76.
- Liao, B.L., Zhang, Z.C., Kou, C.H., and Li, H.B., 2012, Geochemistry of the Shuicheng Permian sodium tra-
- chybasalts in Guizhou Province and constraints on the mantle sources: *Yanshi Xuebao*, v. 28, p. 1238–1250.
- Liu, J.J., Liu, J.M., Gu, X.X., and Lin, L., 1997, Submarine sedimentary exhalative (SEDEX) origin of disseminated gold deposits in SW Guizhou [in Chinese with English abstract]: *Chinese Science Bulletin*, v. 42, p. 2126–2127, <https://doi.org/10.1360/CSB1997-42-19-2126>.
- Lo, C., Chung, S., Lee, T., and Wu, G., 2002, Age of the Emeishan flood magmatism and relations to Permian–Triassic boundary events: *Earth and Planetary Science Letters*, v. 198, p. 449–458, [https://doi.org/10.1016/S0012-821X\(02\)00535-6](https://doi.org/10.1016/S0012-821X(02)00535-6).
- Mao, J.W., Wang, Z.L., Li, H.M., Wang, C.Y., Chen, Y.C., 2003, Carbon and oxygen isotope components in the Permian basalt-hosted copper deposit in Ludian area, Yunnan [in Chinese with English abstract]: *Implication for the mineralization process: Geological Reviews*, v. 49, no. 6, p. 611–615, <https://doi.org/10.16509/j.georeview.2003.06.009>.
- Ohmoto, H., 1972, Systematics of sulfur and carbon isotopes in hydrothermal ore deposits: *Economic Geology*, v. 67, p. 551–578, <https://doi.org/10.2113/gsecongeo.67.5.551>.
- Pi, Q.H., Hu, R.Z., Xiong, B., Li, Q.L., and Zhong, R.C., 2017, In situ SIMS U–Pb dating of hydrothermal rutile: Reliable age for the Zhesang Carlin-type gold deposit in the golden triangle region, SW China: *Mineralium Deposita*, v. 52, p. 1179–1190, <https://doi.org/10.1007/s00126-017-0715-y>.
- Pitcairn, I., 2011, Background concentrations of gold in different rock types: *Transactions of the Institution of Mining and Metallurgy, Section B: Applied Earth Science*, v. 120, p. 31–38, <https://doi.org/10.1179/1743275811Y.0000000021>.
- Qian, G., Xia, F., Brugger, J., Skinner, W., Bei, J., Chen, G., and Pring, A., 2011, Replacement of pyrrhotite by pyrite and marcasite under hydrothermal conditions up to 220 °C: An experimental study of reaction textures and mechanisms: *The American Mineralogist*, v. 96, p. 1878–1893, <https://doi.org/10.2138/am.2011.3691>.
- Ren, Z.Y., Wu, Y.D., Zhang, L., Nichols, A.R.L., Hong, L.B., Zhang, Y.H., Zhang, Y., Liu, Y.Q., and Xu, Y.G., 2017, Primary magmas and mantle sources of Emeishan basalts constrained from major element, trace element and Pb isotope compositions of olivine-hosted melt inclusions: *Geochimica et Cosmochimica Acta*, v. 208, p. 63–85, <https://doi.org/10.1016/j.gca.2017.01.054>.
- Rye, R.O., and Ohmoto, H., 1974, Sulfur and carbon isotopes and ore genesis: A review: *Economic Geology*, v. 69, p. 826–842, <https://doi.org/10.2113/gsecongeo.69.6.826>.
- Seal, R.R., II, 2006, Sulfur isotope geochemistry of sulfide minerals: *Reviews in Mineralogy and Geochemistry*, v. 61, p. 633–677, <https://doi.org/10.2138/rmg.2006.61.12>.
- Shellnutt, J.G., 2014, The Emeishan large igneous province: A synthesis: *Geoscience Frontiers*, v. 5, p. 369–394, <https://doi.org/10.1016/j.gsf.2013.07.003>.
- Shellnutt, J.G., Pham, T.T., Denyszyn, S.W., Yeh, M.W., and Tran, T.A., 2020, Magmatic duration of the Emeishan large igneous province: Insight from northern Vietnam: *Geology*, v. 48, p. 457–461, <https://doi.org/10.1130/G47076.1>.
- Sisson, T.W., 2003, Native gold in a Hawaiian alkalic magma: *Economic Geology*, v. 98, p. 643–648, <https://doi.org/10.2113/gsecongeo.98.3.643>.
- Song, X.Y., Zhou, M.F., Cao, Z.M., Sun, M., and Wang, Y.L., 2003, Ni–Cu–(PGE) magmatic sulfide deposits in the Yangliuping area, Permian Emeishan igneous province, SW China: *Mineralium Deposita*, v. 38, p. 831–843, <https://doi.org/10.1007/s00126-003-0362-3>.
- Su, W.C., Heinrich, C.A., Pettko, T., Zhang, X.C., Hu, R.Z., and Xia, B., 2009, Sediment hosted gold deposits in Guizhou, China: Products of wall-rock sulfidation by deep crustal fluids: *Economic Geology*, v. 104, p. 73–93, <https://doi.org/10.2113/gsecongeo.104.1.73>.
- Su, W.C., Zhang, H.T., Hu, R.Z., Ge, X., Xia, B., Chen, Y.Y., and Zhu, C., 2012, Mineralogy and geochemistry of gold-bearing arsenian pyrite from the Shuiyindong Carlin-type gold deposit, Guizhou, China: Implications for gold depositional processes: *Mineralium Deposita*,

- v. 47, p. 653–662, <https://doi.org/10.1007/s00126-011-0328-9>.
- Su, W.C., Dong, W.D., Zhang, X.C., Shen, N.P., Hu, R.Z., Hofstra, A.H., and Cheng, L.Z., 2018, Carlin-type gold deposits in the Dian-Qian-Gui “Golden Triangle” of Southwest China, in Muntean, J.L., ed., Diversity in Carlin-Style Gold Deposits: Society of Economic Geologists, *Reviews in Economic Geology*, v. 20, p. 157–185, <https://doi.org/10.5382/rev.20.05>.
- Tao, Y., Li, C.S., Hu, R.Z., Ripley, E.M., Du, A.D., and Zhong, H., 2007, Petrogenesis of the Pt–Pd mineralized Jinbaoshan ultramafic intrusion in the Permian Emeishan Large Igneous Province, SW China: Contributions to Mineralogy and Petrology, v. 153, p. 321–337, <https://doi.org/10.1007/s00410-006-0149-5>.
- Tao, Y., Putirka, K., Hu, R.Z., and Li, C.S., 2015, The magma plumbing system of the Emeishan large igneous province and its role in basaltic magma differentiation in a continental setting: *The American Mineralogist*, v. 100, p. 2509–2517, <https://doi.org/10.2138/am-2015-4907>.
- Tassara, S., González-Jiménez, J.M., Reich, M., Schilling, M.E., Morata, D., Begg, G., Saunders, E., Griffin, W.L., O’Reilly, S.Y., Grégoire, M., Barra, F., and Corgne, A., 2017, Plume-subduction interaction forms large auriferous provinces: *Nature Communications*, v. 8, p. 843, <https://doi.org/10.1038/s41467-017-00821-z>.
- Wang, Q.F., and Groves, D., 2018, Carlin-style gold deposits, Youjiang Basin, China: Tectono-thermal and structural analogues of the Carlin-type gold deposits, Nevada, USA: *Mineralium Deposita*, v. 53, p. 909–918, <https://doi.org/10.1007/s00126-018-0837-x>.
- Webber, A.P., Roberts, S., Taylor, R.N., and Pitcairn, I.K., 2013, Golden plumes: Substantial gold enrichment of oceanic crust during ridge-plume interaction: *Geology*, v. 41, p. 87–90, <https://doi.org/10.1130/G33301.1>.
- Wei, D.T., Xia, Y., Gregory, D.D., Steadman, J.A., Tan, Q.P., Xie, Z.J., and Liu, X.J., 2020, Multistage pyrites in the Nibao disseminated gold deposit, southwestern Guizhou province, China: Insights into the origin of Au from textures, in situ trace elements, and sulfur isotope analyses: *Ore Geology Reviews*, v. 122, <https://doi.org/10.1016/j.oregeorev.2020.103446>.
- Wilshire, H.G., and Shervais, J.W., 1975, Al-augite and Cr-diopside ultramafic xenoliths in basaltic rocks from the western United States: *Physics and Chemistry of the Earth*, v. 9, p. 257–272, [https://doi.org/10.1016/0079-1946\(75\)90021-X](https://doi.org/10.1016/0079-1946(75)90021-X).
- Wu, Y.F., Evans, K., Li, J.W., Fougereuse, D., Large, R.R., and Guagliardo, P., 2019, Metal remobilization and ore-fluid perturbation during episodic replacement of auriferous pyrite from an epizonal orogenic gold deposit: *Geochimica et Cosmochimica Acta*, v. 245, p. 98–117, <https://doi.org/10.1016/j.gca.2018.10.031>.
- Xie, Z.J., Xia, Y., Cline, J.S., Pribil, M.J., Koenig, A., Tan, Q.P., Wei, D.T., Wang, Z.P., and Yan, J., 2018, Magmatic origin for sediment-hosted Au deposits, Guizhou Province, China: In situ chemistry and sulfur isotope composition of Pyrites, Shuiyindong and Jinfeng deposits: *Economic Geology*, v. 113, p. 1627–1652, <https://doi.org/10.5382/econgeo.2018.4607>.
- Xu, H., Gao, J.B., Yang, R.D., Feng, K.N., Wang, L.B., and Chen, J., 2021, Metallogenic mechanism of large manganese deposits from Permian manganese ore belt in western South China Block: New mineralogical and geochemical evidence: *Ore Geology Reviews*, v. 132, <https://doi.org/10.1016/j.oregeorev.2021.103993>.
- Xu, T., Zhang, Z.J., Liu, B.F., Chen, Y., Zhang, M.H., Tian, X.B., Xu, Y.G., and Teng, J.W., 2015, Crustal velocity structure in the Emeishan large igneous province and evidence of the Permian mantle plume activity: *China Earth Sciences*, v. 58, p. 1133–1147, <https://doi.org/10.1007/s11430-015-5094-6>.
- Xu, Y.G., He, B., Chung, S.L., Menzies, M.A., and Frey, F.A., 2004, Geologic, geochemical, and geophysical consequences of plume involvement in the Emeishan flood-basalt province: *Geology*, v. 32, p. 917–920, <https://doi.org/10.1130/G20602.1>.
- Yan, H., Pi, D.H., Jiang, S.Y., Hao, W.D., Mänd, K., Robbins, L.J., Li, L., and Konhauser, K.O., 2020, New constraints on the onset age of the Emeishan LIP volcanism and implications for the Guadalupian mass extinction: *Lithos*, v. 360–361, <https://doi.org/10.1016/j.lithos.2020.105441>.
- Yan, J., Hu, R.Z., Liu, S., Lin, Y.T., Zhang, J.C., and Fu, S.L., 2018, NanoSIMS element map-ping and sulfur isotope analysis of Au-bearing pyrite from Lannigou Carlin-type Au deposit in SW China: New insights into the origin and evolution of Au-bearing fluids: *Ore Geology Reviews*, v. 92, p. 29–41, <https://doi.org/10.1016/j.oregeorev.2017.10.015>.
- Yao, J.H., Zhu, W.G., Li, C.S., Zhong, H., Yu, S., Ripley, E.M., and Bai, Z.J., 2019, Olivine O isotope and trace element constraints on source variation of picrites in the Emeishan flood basalt province, SW China: *Lithos*, v. 338, p. 87–98, <https://doi.org/10.1016/j.lithos.2019.04.019>.
- Zhang, Z.C., Mao, J.W., Wang, F.S., and Pirajno, F., 2006a, Native Au and native copper grains enclosed by olivine phenocrysts in a picrite lava of the Emeishan large province, SW China: *The American Mineralogist*, v. 91, p. 1178–1183, <https://doi.org/10.2138/am.2006.1888>.
- Zhang, Z.C., Mahoney, J.J., Mao, J.W., and Wang, F.S., 2006b, Geochemistry of picritic and associated basalt flows of the Western Emeishan Flood Basalt province, China: *Journal of Petrology*, v. 47, p. 1997–2019, <https://doi.org/10.1093/ptrology/egl034>.
- Zhang, Z.C., Zhi, X.C., Chen, L.L., Saunders, A.D., and Reichow, M.K., 2008, Re-Os isotopic compositions of picrites from the Emeishan flood basalt province, China: *Earth and Planetary Science Letters*, v. 276, p. 30–39, <https://doi.org/10.1016/j.epsl.2008.09.005>.
- Zhang, Z.C., Mao, J.W., Saunders, A.D., Ai, Y., Li, Y., and Zhao, L., 2009, Petrogenetic modeling of three mafic-ultramafic layered intrusions in the Emeishan large igneous province, SW China, based on isotopic and bulk chemical constraints: *Lithos*, v. 113, p. 369–392, <https://doi.org/10.1016/j.lithos.2009.04.023>.
- Zhong, Y.T., He, B., Mundil, R., and Xu, Y.G., 2014, CA-TIMS zircon U–Pb dating of felsic ignimbrite from the Binchuan section: implications for the termination age of Emeishan large igneous province: *Lithos*, v. 204, p. 14–19, <https://doi.org/10.1016/j.lithos.2014.03.005>.
- Zhou, J.X., Huang, Z.L., Zhou, M.F., Zhu, X.K., and Muchez, P., 2014, Zinc, sulfur and lead isotopic variations in carbonate-hosted Pb–Zn sulfide deposits, Southwest China: *Ore Geology Reviews*, v. 58, p. 41–54, <https://doi.org/10.1016/j.oregeorev.2013.10.009>.
- Zhou, M.F., Robinson, P.T., Leshner, C.M., Keays, R.R., Zhang, C.J., and Malpas, J., 2005, Geochemistry, petrogenesis and metallogenesis of the Panzhihua gabbroic layered intrusion and associated Fe–Ti–V oxide deposits, Sichuan Province, SW China: *Journal of Petrology*, v. 46, p. 2253–2280, <https://doi.org/10.1093/ptrology/egi054>.
- Zhu, J., Zhang, Z.C., Reichow, M.K., Li, H.B., Cai, W.C., and Pan, R.H., 2018, Weak vertical surface movement caused by the ascent of the Emeishan mantle anomaly: *Journal of Geophysical Research: Solid Earth*, v. 123, p. 1018–1034, <https://doi.org/10.1002/2017JB015058>.
- Zhu, J., Zhang, Z.C., Santosh, M., and Jin, Z.L., 2020, Carlin-style gold province linked to the extinct Emeishan plume: *Earth and Planetary Science Letters*, v. 530, <https://doi.org/10.1016/j.epsl.2019.115940>.
- Zhu, J., Zhang, Z.C., Santosh, M., Tan, S.C., and Jin, Z.L., 2021, Submarine basaltic eruptions across the Guadalupian-Lopingian transition in the Emeishan large igneous province: Implication for end-Guadalupian extinction of marine biota: *Gondwana Research*, v. 92, p. 228–238, <https://doi.org/10.1016/j.gr.2020.12.025>.
- Zhuo, Y.Z., Hu, R.Z., Xiao, J.F., Zhao, C.H., Huang, Y., Yan, J., Li, J.W., Gao, W., and Li, J.X., 2019, Trace elements and C–O isotopes of calcite from Carlin-type gold deposits in the Youjiang basin, SW China: Constraints on ore-forming fluid compositions and sources: *Ore Geology Reviews*, v. 113, <https://doi.org/10.1016/j.oregeorev.2019.103067>.

SCIENCE EDITOR: MIHAI DUCEA
ASSOCIATE EDITOR: JEAN BÉDARD

MANUSCRIPT RECEIVED 18 MARCH 2022
REVISED MANUSCRIPT RECEIVED 17 MAY 2022
MANUSCRIPT ACCEPTED 9 JUNE 2022

Printed in the USA